Stem Cell Research & Therapy

RESEARCH

Open Access

Empagliflozin-pretreated BMSC exosomes attenuate myocardial ischemia-reperfusion injury by enhancing atad3a/pink1-dependent mitophagy

Yuling Jing[1], Ying Cai[1], Qiuting Li[1,2], Zaiyong Zheng[1], Haiqiong Yang[1], Yang Yu[1,2,3,4*] and Chunxiang Zhang[1,2,3,4*]

Abstract

Background and objectives Mounting evidence demonstrates that exosomes derived from mesenchymal stem cells (MSCs) can mitigate myocardial ischemia-reperfusion injury (MIRI). However, the therapeutic potential of untreated MSC-derived exosomes remains limited. Here, we investigate whether exosomes derived from sodium-glucose co-transporter 2 inhibitor (SGLT2i)-pretreated MSCs exhibit enhanced cardioprotective effects against MIRI and elucidate the underlying mechanisms.

Methods and results Mouse bone marrow-derived MSCs (BMSCs) were pretreated with the SGLT2 inhibitor empagliflozin (EMPA), and the secreted exosomes (EMPA-EXO) were isolated. Primary neonatal cardiomyocytes were co-cultured with EMPA-EXO or untreated exosomes (EXO) for 24 h before hypoxia-reoxygenation (H/R) injury. In the MIRI mice, EXO or EMPA-EXO were delivered via intramyocardial injection. EMPA pretreatment significantly augmented exosome secretion from BMSCs by modulating the expression of Alix, nsmase2, and RAB27a. In vitro, both EXO and EMPA-EXO enhanced cardiomyocyte viability, attenuated cellular damage, and suppressed apoptosis following H/R injury. In vivo, EMPA-EXO and EXO administration improved cardiac function, reduced myocardial apoptosis, and diminished infarct size in MIRI mice mice. Mechanistically, Western blot and transmission electron microscopy (TEM) revealed that both exosome types upregulated ATAD3A expression, thereby activating PINK1/PARKIN-mediated mitophagy and ameliorating cardiomyocyte injury.

Conclusion Our findings demonstrated that EMPA enhanced exosome secretion from BMSCs. Both EMPA-EXO and EXO attenuated MIRI by upregulating ATAD3A, which promoted PINK1/PARKIN-dependent mitophagy. Notably, EMPA-EXO exhibitd superior therapeutic efficacy compared to EXO, suggesting a promising strategy for optimizing MSC-derived exosome therapy in ischemic heart disease.

Keywords Empagliflozin, Myocardial ischemia-reperfusion injury, Exosomes, Mitophagy

*Correspondence:
Yang Yu
dr.yangyuself@gmail.com
Chunxiang Zhang
zhangchx999@163.com; zcxteam@163.com

Full list of author information is available at the end of the article

Graphical abstract

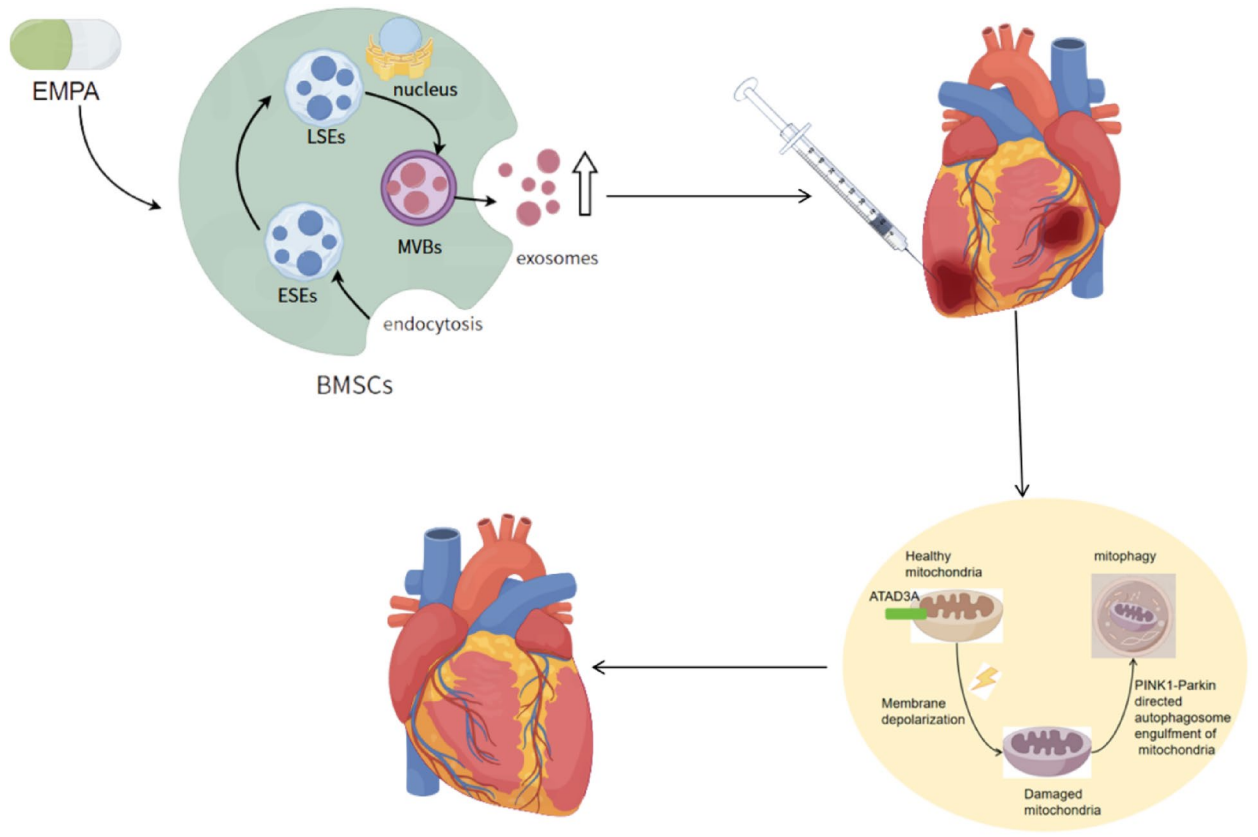

Introduction

Ischemic cardiomyopathy (ICM) represents a leading cause of global cardiovascular mortality, with reperfusion therapy remaining the cornerstone of clinical management. However, reperfusion-induced ionic imbalance and reactive oxygen species (ROS) overproduction often exacerbate cardiomyocyte death—a phenomenon termed myocardial ischemia/reperfusion injury (MIRI). Despite advances, current pharmacotherapies for ICM exhibit limited efficacy and carry risks of bleeding, hepatotoxicity, and arrhythmias [1], underscoring the urgent need for novel therapeutic strategies.

Mesenchymal stem cells (MSCs) have emerged as promising candidates for regenerative therapy, with their benefits largely attributed to paracrine signaling rather than direct differentiation [2]. Exosomes, the key paracrine mediators of MSCs [3], mitigate ICM by reducing apoptosis [4, 5], suppressing inflammation [6], and enhancing angiogenesis [7]. However, the clinical translation of MSC-derived exosomes (MSCs-EXO) is hindered by their low natural yield and suboptimal potency. Pharmacological preconditioning—exemplified by atorvastatin and tanshinone IIA [8, 9]—offers a pragmatic approach to enhance MSCs-EXO efficacy.

Sodium-glucose cotransporter 2 inhibitors (SGLT2is), a new class of glucose-lowering agents, have been widely adopted in clinical practice. Substantial evidence from clinical and preclinical studies demonstrates their beneficial effects in heart failure [10], ischemic cardiomyopathy [11], and arrhythmia [12]. These agents exhibit low cellular toxicity and have been shown to ameliorate multiple pathological processes in cardiomyocytes, including mitochondrial dysfunction, disruption of ion homeostasis, inflammatory responses, oxidative stress, ventricular remodeling, and impaired autophagy. Recent studies further indicate that combining MSCs with SGLT2is can significantly improve outcomes in diabetic neuropathy and nephropathy [13]. Chi et al. found that empagliflozin (EMPA) could increase the cell viability, migration ability, and inhibit apoptosis and senescence of MSCs [14]. However, it remains unclear whether SGLT2is exert their therapeutic effects on MIRI partially through modulation of MSCs-EXO.

Mitochondrial dysfunction is a hallmark of MIRI, where mitophagy—the selective clearance of damaged mitochondria—plays a pivotal homeostatic role. The mitochondrial protein ATAD3A, known to regulate dynamics and metabolism, exhibits context-dependent

effects on mitophagy: it suppresses PINK1/Parkin-mediated mitophagy in cancer and cerebral ischemia [15–17] but paradoxically requires PINK1 for mitophagy inhibition in fatty liver disease [18]. Whether ATAD3A governs this pathway in ICM is unknown.

Here, we investigate the hypothesis that EMPA-preconditioned MSCs secrete exosomes with enhanced cardioprotective efficacy against MIRI, and elucidate the role of the ATAD3A/PINK1 axis in regulating mitophagy.

Materials and methods

Reporting guidelines

The work has been reported in line with the ARRIVE guidelines 2.0.

Animals

Considering the protective effect of estrogen on the heart, male C57BL/6 mice was used in this experiment. 100 male C57BL/6 mice (8 weeks old) were obtained from HUACHUANG SINO Pharmaceutical Technology Co., Ltd. (Jiangsu, China). All mice were fed in SPF room. The feeding room was kept quiet, maintained at approximately 25 °C with 40–50% humidity, and a 12-h day and night cycle. Feed and water intake of the mice were not restricted, and the padding was changed regularly. All animal procedures conformed to the Guide for the Care and Use of Laboratory Animals published by the US National Institute of Health (8th edition, 2011) and were approved by the Institutional Animal Care and Treatment Committee of Southwest Medical University, China. The ethical number is No. 2,020,255. Mice were randomized into four groups ($n = 25$ in each group): Control, I/R (ischemia-reperfusion + PBS), EXO (I/R + BMSC-derived exosomes), EMPA-EXO (I/R + empagliflozin-pretreated BMSC-derived exosomes).

Exosome isolation and characterization

Mouse bone marrow mesenchyml stem cell (BMSCs) (Procell Life Science & Technology Co., Ltd., Wuhan) were cultured in DMEM with 10% FBS and 1% penicillin-streptomycin. To identify the optimal concentration of empagliflozin (EMPA), we treated BMSCs with varying concentrations of EMPA (0.25 μM, 0.5 μM, and 1 μM). We evaluated the protein levels of key regulators of exosome biogenesis—Alix, nSMase2, and RAB27a. Based on the most pronounced upregulation of these markers, 1 μM was selected as the optimal concentration for EMPA treatment. At 80% confluency, cells were treated with 1 μM EMPA or vehicle (serum-free DMEM) for 24 h. Exosomes were isolated from supernatants using a commercial kit (Umibio, UR52121) and characterized by: Transmission electron microscopy (TEM) (morphology), Western blot (CD9/CD63/CD81, Calnexin), Nanoparticle tracking analysis (NTA)(particle size distribution), BCA assay (protein quantification).

Exosome uptake assay

PKH67-labeled exosomes were incubated with HL-1 cardiomyocytes (Procell Life Science & Technology Co., Ltd., Wuhan) for 24 h. Cells were fixed (4% PFA, 20 min), stained with DAPI, and imaged by fluorescence microscopy.

Hypoxia-reoxygenation (H/R) model

The cell experiments were divided into 4 groups(n = 25 in each group): NC, H/R (H/R + PBS), EXO (H/R + BMSC-derived exosomes), EMPA-EXO (H/R + empagliflozin-pretreated BMSC-derived exosomes). Primary neonatal mouse cardiomyocytes (NMCMs) were isolated as described [19]. After 24 h co-culture with EXO/EMPA-EXO, cells underwent hypoxia (95% N_2/5% CO_2, 6 h) (Thermo STERI-CYCLE i160 CO2 Incubator) followed by reoxygenation (4 h).

Myocardial I/R model and exosome delivery

Mice were anesthetized (5% isoflurane), intubated, and subjected to LAD ligation (7 – 0 suture, 30 min ischemia). Exosomes (100 μg/mouse) or PBS were injected intramyocardially at five sites (apex, infarct, border zone) prior to reperfusion. Sham controls underwent thoracotomy without ligation.When sampling, the mice were first anesthetized with isoflurane inhalation and then sacrificed by necking.

Echocardiography

Cardiac function was assessed 24 h post-reperfusion (Vevo2100, FUJIFILM). Parameters included: the left anterior ventricular wall during diastole (LVAWd), the anterior wall of the left ventricle during systole (LVAWs), the left ventricular diameter during diastole (LVIDd), the left ventricular diameter during systole (LVIDs), the left ventricular ejection fraction (LVEF), the left ventricular fractional shortening (LVFS).

MTT cell viability assay

HL-1 cardiomyocytes were plated in 96-well plates at a density of 1×10^4-5×10^4 cells/well and allowed to adhere overnight. Following hypoxia-reoxygenation (H/R) treatment, cell viability was assessed using the MTT assay. Briefly, MTT (3-(4,5-dimethylthiazol-2-yl)-2,5-diphenyltetrazolium bromide) was added to each well at a final concentration of 0.5 mg/mL and incubated for 2 h at 37 °C under 5% CO_2. The formazan crystals formed by viable cells were solubilized in 100 μL DMSO with gentle agitation (10–15 min). Absorbance was measured at 570 nm using a microplate reader, with reference wavelength set at 630 nm. Cell viability was calculated as:

Viability (%) = [(OD_{570} sample - OD_{570} blank)/(OD_{570} control - OD_{570} blank)] × 100.

LDH activity assay

Cell culture supernatants were centrifuged at 1,000 × g for 10 min at 4 °C to remove cellular debris. Cleared supernatants were immediately used. Working solution was freshly prepared by mixing assay buffer with NAD^+ substrate at a 5:1 ratio (v/v). Load the samples according to Table 1. Absorbance at 340 nm was recorded every 30 s for 3 min using a microplate reader pre-equilibrated to 37 °C. LDH activity (U/L)=($\Delta A340$,sample/min – $\Delta A340$,blank/min)/6.22 × 200/5 × 1000.

HE staining

Isolated hearts were fixed in 4% paraformaldehyde (PFA) for 48 h at 4 °C, then processed through a graded ethanol series (70% to 100%) and xylene before paraffin embedding. Tissue Sects. (5–10 μm) were cut using a microtome, mounted on slides, and baked at 62 °C for 100 min. After deparaffinization and rehydration, sections were stained with hematoxylin (6 min) and eosin (2 min) following standard protocols. Slides were imaged using a bright-field microscope with objective.

TUNEL assay

Myocardial apoptosis was assessed using the TUNEL Apoptosis Detection Kit (Beyotime, C1088). Deparaffinized sections were treated with proteinase K (20 μg/mL, 37 °C, 30 min), then incubated with TUNEL reaction mixture (TdT enzyme: labeling solution = 1:9) for 60 min at 37 °C in the dark. After PBS washing, sections were mounted with anti-fade medium and imaged using fluorescence microscopy (emission: 565 nm). Apoptotic nuclei were quantified with Image J from 5 random fields per sample.

Myocardial infarction assessment (Evans blue/TTC staining)

Following reperfusion, Evans Blue (1%, 1 mL) was perfused via carotid artery to demarcate the area-at-risk (AAR). Hearts were sectioned (1–2 mm) and incubated with 1% TTC (37 °C, 15–30 min, dark). Sections were imaged, and infarct size was calculated with Image J as: AAR/LV (%) = (AAR area/total LV area) × 100, INF/AAR (%) = (TTC-negative area/AAR area) × 100.

Table 1

Component	Test well (μL)	Blank well (μL)
Sample	5	-
ddH_2O	-	5
Working solution	195	195

Western blot

Tissue proteins and cell proteins were extracted using RIPA buffer supplemented with protease/phosphatase inhibitors (1:100). Protein concentration was determined by BCA assay. Proteins (20 μg/lane) were separated by SDS-PAGE (10–12% gels) at 60 V (stacking gel) then 120 V (resolving gel), and transferred to PVDF membranes (300 mA, 90 min, ice bath). Blocked with 5% skim milk for 2 h at room temperature on a low-speed shaker. The membrane was incubated overnight at 4 °C with primary antibodies (ATAD3A: 1:1000, ab317252, abcam; PINK1: 1:2000, proteintech, 23274-1; ALIX: 1:1000, ET1705-74, HUABIO; RAB27A: 1:1000, 66058-1-Ig, proteintech; SMPD2: 1:1000, 15239-1-AP, proteintech; parkin: 1:1000, 14060-1-AP, proteintech; BAX: 1:10000, 60267-1-Ig, proteintech; P62: 1:2000, ab314504, abcam; Lc3B: 1:2000, 43566T, CST; BCL-2: 1:1000, ab196495, abcam; GAPDH: 1:5000, 60004-1-1 g, proteintech). After TBST washes, membranes were incubated with HRP-conjugated secondary antibodies (1:5000, 1.5 h, RT). Signals were detected by ECL (Bio-Rad ChemiDoc) and quantified (Image J).

Immunofluorescence

Dewaxing and hydration of paraffin sections. Adding 20 μg/ml of proteinase K without DNase and acting at 37℃ for 30 min. Washing three times with PBS. Permeation: 0.1%-0.5% Triton X-100/PBS, 10–15 min. Block: 5% BSA or homologous serum, room temperature for 1 h. Diluting ATAD3A with PBS containing 1% BSA at a ratio of 1:200 and incubating overnight at 4 ° C. Washing three times with PBS for 5 min and incubating the fluorescent secondary antibody at room temperature in the dark for 1 h. Sealing the plate with an anti-quenching mounting agent containing DAPI. Fluorescence microscope observation and photography.

Flow cytometry for apoptotic cell detection

Flow cytometry was performed using the Apoptosis Kit of 4 A Biotech (China Suzhou, FXP018-100). After H/R treatment, the cells were digested from the culture dish using trypsin without EDTA. The cells were transferred to a 15 ml centrifuge tube, centrifuged at 1000 rpm for 3 min, and the supernatant was discarded. The cells were resuspended in PBS and washed twice. Blank tubes, single staining tubes, and experimental tubes were set up. The cells were diluted 1:3 with binding buffer in deionized water and resuspended with 1x binding buffer to adjust the concentration to $1–5 \times 10^6$/ml. 100 μl of cell suspension was added to a 5 ml flow cytometry tube, 5 μl of Annexin V/FITC was added and mixed well, and incubated at room temperature in the dark for 5 min. 10 μl of 20 ug/ml propidium iodide solution (PI) was added and

400 µl PBS was added immediately for flow cytometry detection.

ROS probe

Diluting the ROS probe (Solarbio/D6470-25 mg) in serum-free medium to 10 µmol/L. Adding it to the H/R cells culture dish, incubating in a normal incubator under dark conditions for 20 min, washing twice with PBS, and observing and photograph under a fluorescence microscope.

Statistical analysis

Immunofluorescence and WB were measured using image J. Prismchs was used for data processing, and the measurement data were expressed in the form of $X \pm SD$. T-test and Two-way repeated measures ANOVA were used for comparison between groups, and P less than 0.05 was considered statistically significant.

Results

Characterization and uptake of exosomes

TEM revealed that both EXO and EMPA-EXO exhibited characteristic spherical morphology(Fig. 1A). NTA demonstrated that EMPA pretreatment increased exosome yield (EMPA-EXO: 9.7×10^7 particles/mL vs. EXO: 6.9×10^7 particles/mL) while maintaining comparable size distributions (peak diameters: 114.6 ± 3.2 nm vs. 112.6 ± 2.8 nm; Fig. 1B). PKH67-labeling confirmed efficient uptake of both exosome types by cardiomyocytes within 24 h (Fig. 1C). Western blot (WB) analysis showed that CD9, CD63 and CD81 proteins expressed in exosomes, while calnexin protein expressed in extremely low levels (Fig. 1D).

EMPA enhanced exosome biogenesis in BMSCs

EMPA treatment (1 µM) significantly augmented exosome secretion from BMSCs, evidenced by: particle concentration ($P < 0.0001$; Fig. 2A) and protein content ($P < 0.0001$; Fig. 2B) increased. Mechanistically, EMPA upregulated key exosome biogenesis regulators (Fig. 2C): Alix ($P < 0.0001$), nSMase2 ($P < 0.001$), RAB27a ($P < 0.0001$). These results suggested that EMPA could promote EXO secretion.

EMPA-EXO attenuated H/R injury in cardiomyocytes

In NMCMs subjected to H/R, EMPA-EXO reduced BAX ($P < 0.05$), increased Bcl-2 ($P < 0.01$) vs. EXO (Fig. 3A) and decreased late apoptotic HL-1 cells ($P < 0.0001$) and total apoptotic HL-1 cells ($P < 0.01$) (Fig. 3B).In addition, EMPA-EXO improved cell viability ($P < 0.05$; Fig. 3C), reduced LDH release ($P < 0.01$; Fig. 3D) and lowered ROS vs. EXO ($P < 0.01$; Fig. 3E).

EMPA-EXO ameliorated myocardial ischemia-reperfusion injury

In I/R mices (30 min ischemia/24 h reperfusion), although EXO and EMPA-EXO did not show significant differences in improving LVAWd, LVAWs, LVIDd, and LVIDs compared to the I/R group, they could significantly improve cardiac function(Fig. 4A) in I/R mice, as indicated by significantly increased LVEF and LVFS. Moreover, EMPA-EXO had a more significant therapeutic effect than EXO ($P < 0.01$; $P < 0.01$). HE staining(Fig. 4B

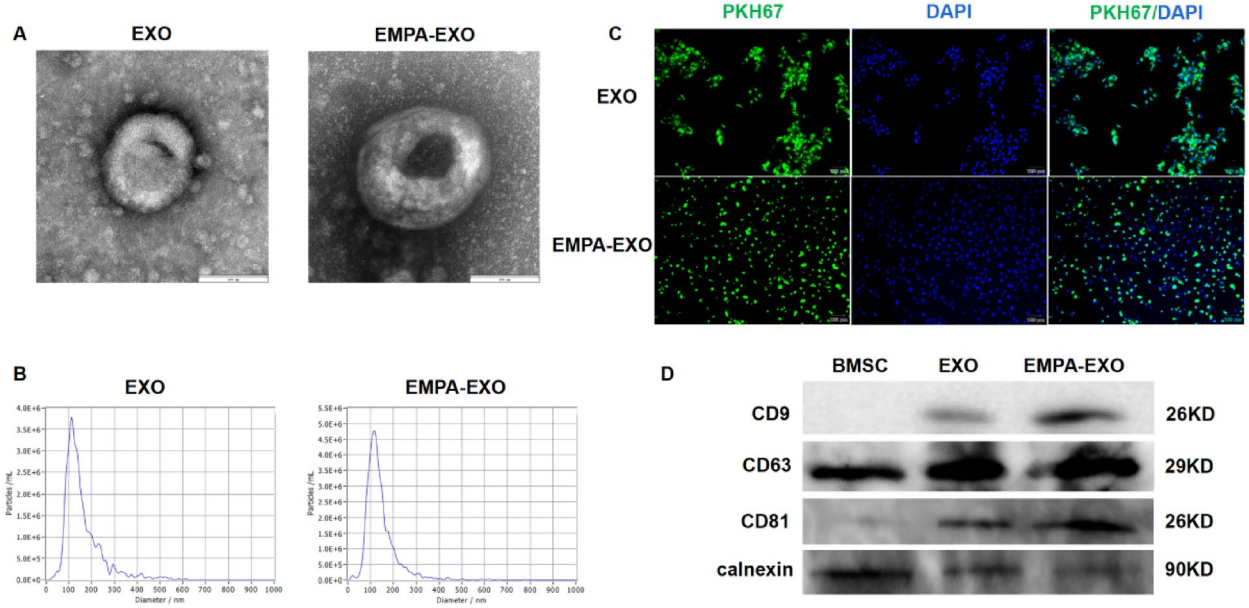

Fig. 1 Characterization and Uptake of Exosomes. **A** Exosome morphology under TEM. **B** NTA: concentration and particle size distribution. **C** exosome Uptake Assay. **D** marker proteins of exosomes

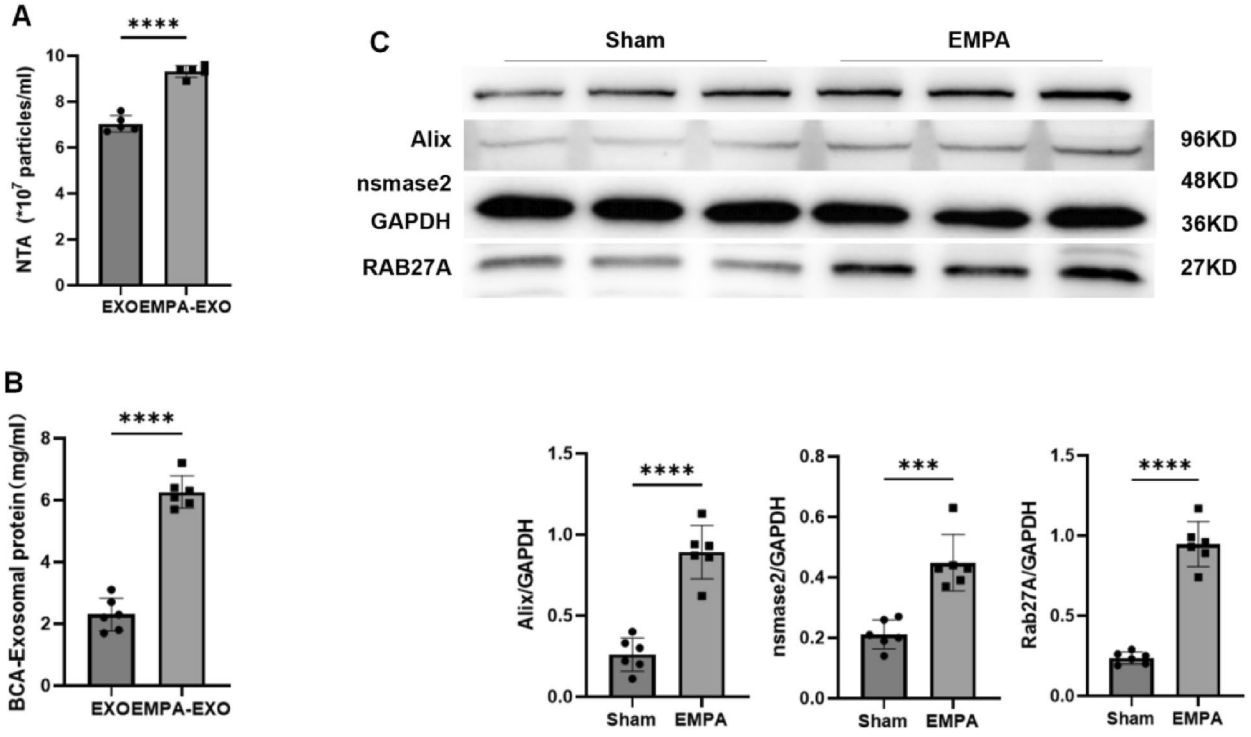

Fig. 2 EMPA Enhanced Exosome Biogenesis in BMSCs. **A**, **B** Exosome particle and protein concentration. **C** EMPA upregulated key exosome biogenesis regulators: Alix, nSMase2, RAB27a

) suggested that compared to EXO, EMPA-EXO could further ameliorate inflammatory cell infiltration, myocardial edema, myocardial cell vacuolization, myocardial fiber distortion and rupture, and disordered arrangement in I/R mice. TUNEL ($P<0.05$; Fig. 4C) and WB (BAX, $P<0.001$; Bcl-2, $P<0.05$; Fig. 4D) indicated that EMPA-EXO had a better effect on ameliorating myocardial apoptosis in I/R mice than EXO. The TTC (Fig. 4E) results also indicated that EMPA-EXO could more significantly reduce myocardial infarction area after I/R compared with EXO ($P<0.001$).

EMPA-EXO promoted mitophagy in ischemia-reperfusion cardiomyocytes

MIRI can induce mitochondrial damage. Mitophagy selectively sequesters and degrades damaged or dysfunctional mitochondria within cells, thereby preventing further cellular injury. Studies have reported that ATAD3A can regulate mitophagy by affecting PINK1, but there are few reports on ATAD3A in MIRI model. Therefore, we investigated the role of ATAD3A in MIRI. WB and immunofluorescence (Fig. 5A and B) showed that the protein level of ATAD3A were decreased in H/R NMCMs ($P<0.001$) and I/R mice myocardial tissues ($P<0.05$; $P<0.001$). To explore the effect of ATAD3A on PINK1 in MIRI, we detected the protein content of PINK1, and the results indicated that PINK1 expression decreased in MIRI($P<0.01$; $P<0.01$), consistent with the trend of ATAD3A (Fig. 5C). Then, we used siRNA of ATAD3A to knockdown ATAD3A in cardiomyocytes and detected PINK1 by WB (Fig. 5D). The results showed that PINK1 decreased along with the decrease of ATAD3A. Subsequently, we explored the effect of EMPA-EXO on mitophagy. Firstly, we explored the effects of EXO and EMPA-EXO on ATAD3A in H/R NMCMs and I/R myocardial tissues. WB and immunofluorescence showed that EXO and EMPA-EXO could significantly increase the expression of ATAD3A in H/R NMCMs and I/R myocardial tissues, and the effect of EMPA-EXO was more significant than that of EXO ($P<0.01$,Fig. 5E; $P<0.001$,Fig. 5F, $P<0.05$,Fig. 5G). WB (Fig. 5E and F) showed that the expressions of PINK1, and PARKIN were significantly decreased in H/R NMCMs ($P<0.0001$, $P<0.01$) and I/R mice myocardial tissues($P<0.0001$, $P<0.0001$). Although in the H/R NMCMs and I/R mice LC3II/LC3I increased($P<0.05$, $P<0.05$), P62 also increased ($P<0.0001$, $P<0.0001$), suggesting that autophagic flux was inhibited. Compared with EXO, EMPA-EXO could further increase the expression of PINK1, PARKIN, LC3II/LC3I, and P62 in NMCMs ($P<0.05$; $P<0.01$; $P<0.01$; $P<0.01$) and I/R myocardial tissues ($P<0.01$; $P<0.05$; $P<0.01$; $P<0.01$). TEM (Fig. 5G) showed that the myocardium of I/R mice was swollen, and the mitochondria were swollen with reduced cristae. EXO and EMPA-EXO significantly improved myocardial edema, and autophagic bodies were clearly visible in

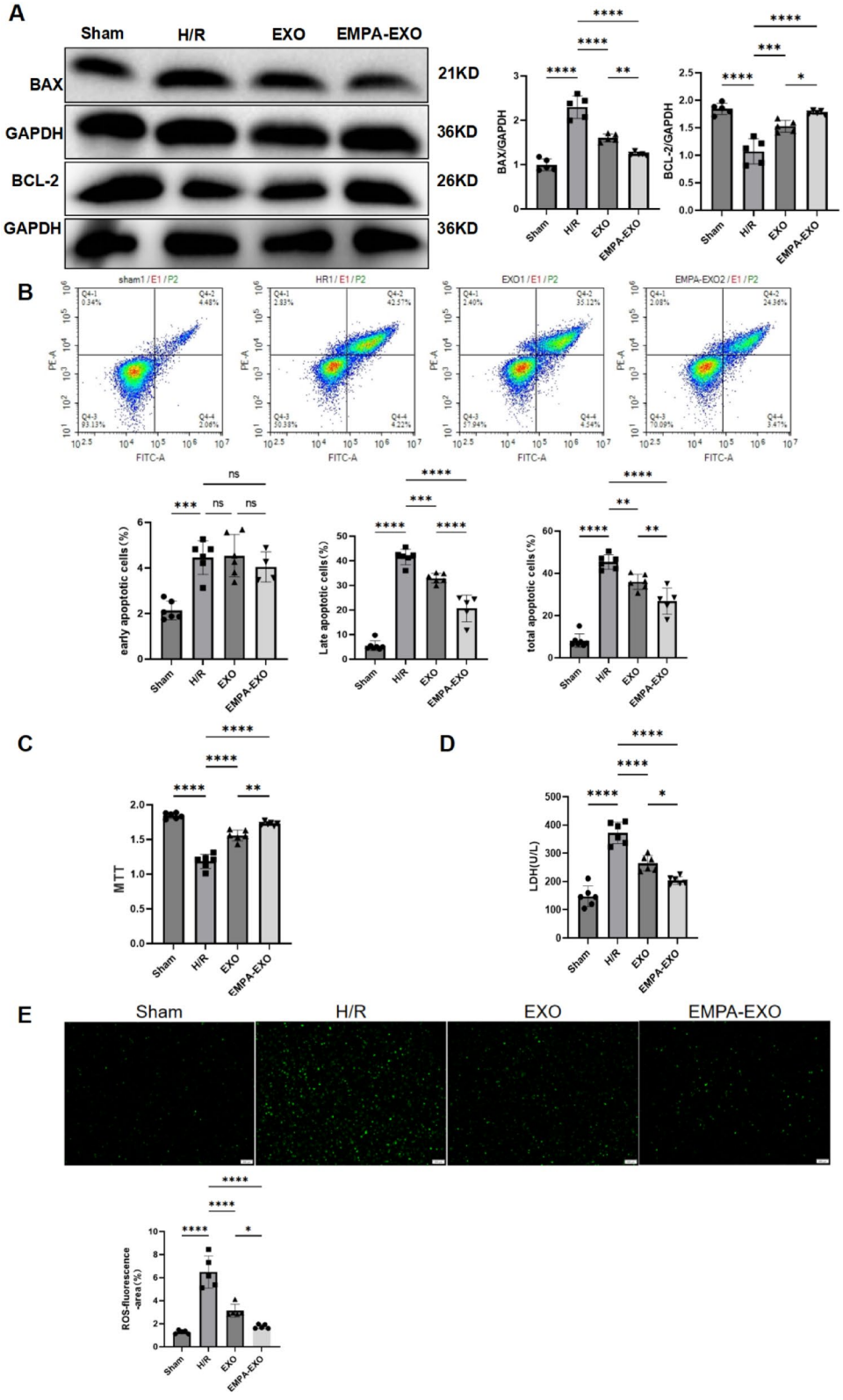

Fig. 3 MPA-EXO Attenuated H/R Injury in Cardiomyocytes. **A**, **B** EMPA-EXO further reduced the apoptosis of H/R cardiomyocytes. **C**, **D**, **E** EMPA-EXO further reduced H/R cardiomyocytes injury

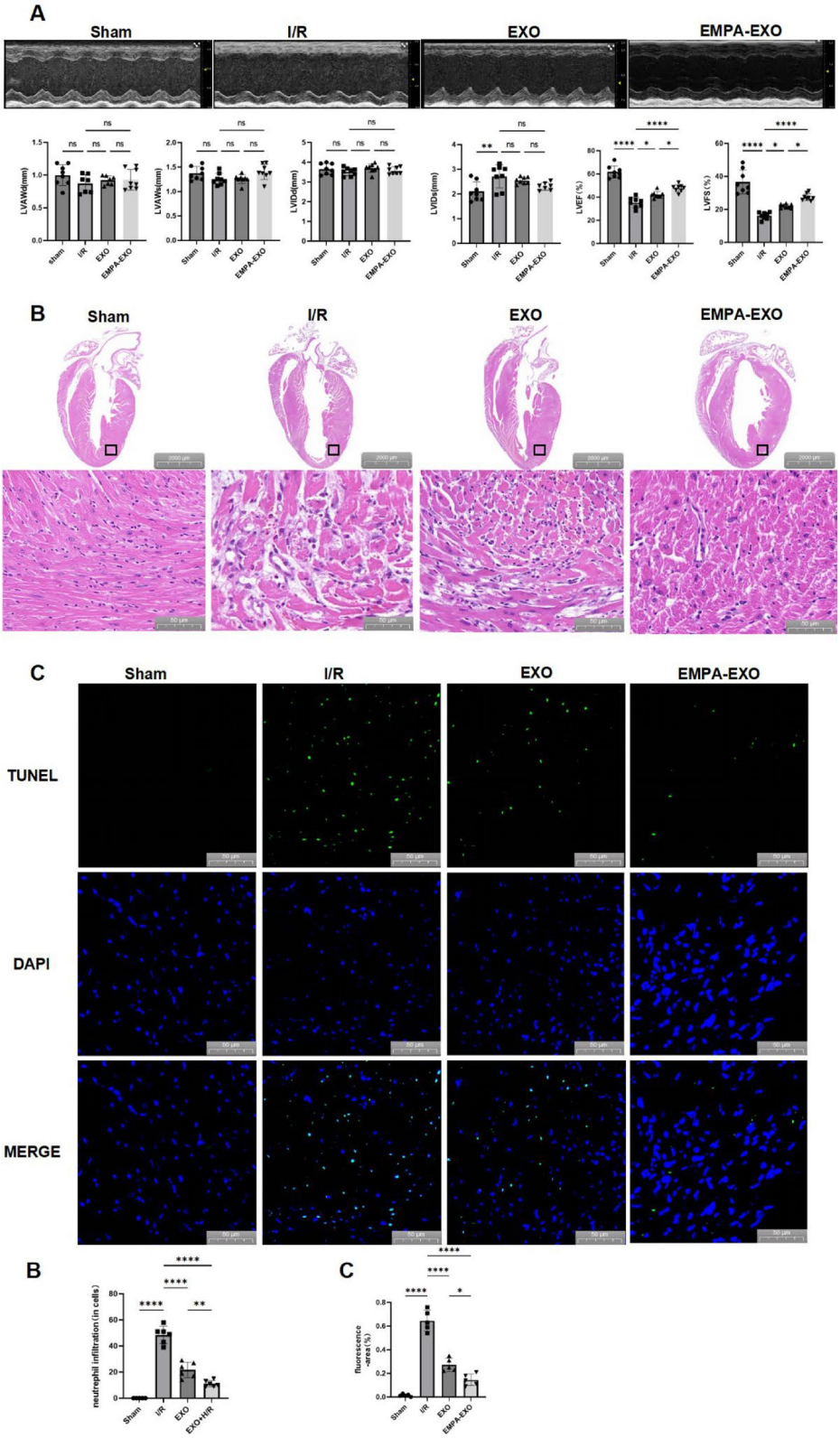

Fig. 4 EMPA-EXO Ameliorated Myocardial Ischemia-Reperfusion Injury. **A** Echocardiography : EMPA-EXO further improved the I/R mice cardiac function. **B HE**: EMPA-EXO further reduced the I/R mice myocardial injury. **D** EMPA-EXO further reduced the I/R mice myocardium apoptosis. **E** EMPA-EXO further reduced the I/R mice myocardial infarct area

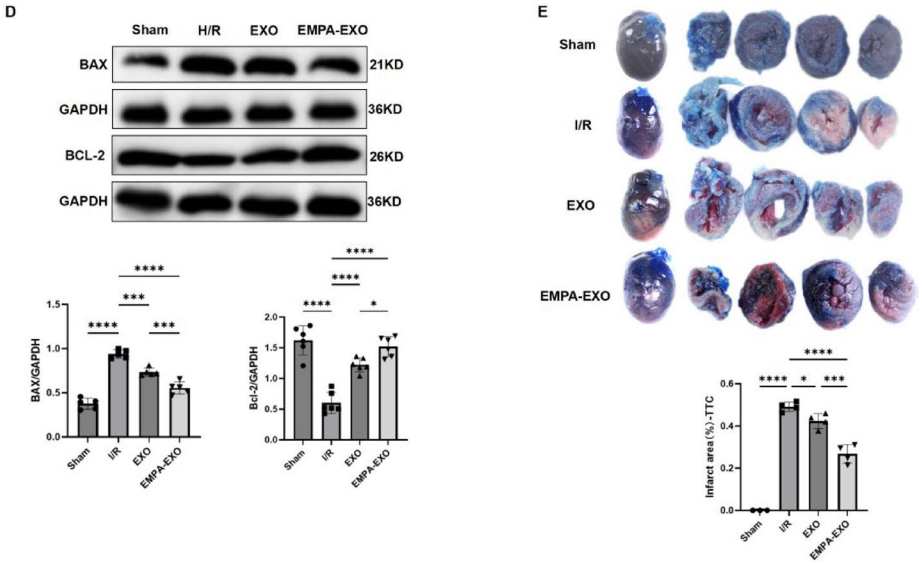

Fig. 4 (continued)

the EXO and EMPA-EXO groups compared with the I/R group, and the effect of EMPA-EXO was more obvious than that of EXO.

Discussion

Our experimental results demonstrated that EMPA-EXO exhibited superior therapeutic efficacy compared to conventional EXO in mitigating MIRI. Specifically, we observed that: (1) EMPA treatment significantly enhanced the secretory capacity of MSCs, leading to increased EXO production; (2) EMPA-EXO confers more pronounced cytoprotective effects in H/R cardiomyocytes in vitro; (3) EMPA-EXO administration resulted in greater improvement in cardiac function and reduced myocardial damage in I/R mice in vivo. (4) The ATAD3A expression was significantly decreased in MIRI, and ATAD3A promoted PINK1/PARKIN-dependent mitophagy. (5) EXO and EMPA-EXO ameliorated MIRI by enhancing mitophagy in H/R cardiomyocytes as well as I/R mice.

Chi et al. suggested that small extracellular vesicles derived from MSCs pretreated with EMPA had a significant myocardial protective effect on ICM [14], we also reached the same conclusion. Our findings demonstrated that both EMPA-EXO and EXO significantly attenuated MIRI by ameliorating cardiomyocytes injury. Accumulating evidence has elucidated diverse cardioprotective mechanisms mediated by BMSCs-EXO, including: Sun et al. demonstrated that BMSCs-EXO suppressed apoptosis in I/R rat myocardium and H/R H9C2 cells via PTEN downregulation and subsequent PI3K/AKT pathway activation [20]. Further mechanistic insight was provided by Li et al., showing BMSCs-EXO-mediated regulation of the PTEN-Akt-mTOR axis effectively curbed excessive autophagy in H/R NMCMs [21]. Additional studies revealed that BMSCs-EXO negatively regulate Gasdermin D expression at both transcriptional and translational levels, consequently mitigating Gasdermin D-dependent pyroptosis and inflammatory responses in both I/R mice and H/R cardiomyocytes [22]. Notably, exosomes derived from alternative sources exhibit distinct protective mechanisms. Human umbilical cord mesenchymal stem cell-derived exosomes (UCMSCs-EXO) have been shown to inhibit ferroptosis in H/R cardiomyocytes through suppression of DMT1 expression [23], expanding the therapeutic repertoire of exosome-based interventions for MIRI.

As the principal energy-generating organelles in cardiomyocytes, mitochondria are essential for maintaining cardiac function. During I/R injury, mitochondria undergo pathological alterations including: swelling, collapse of mitochondrial membrane potential ($\Delta\Psi m$), and electron transport chain dysfunction. These disturbances collectively impair ATP production while promoting reactive oxygen species (ROS) accumulation [24], thereby exacerbating cellular injury. Selective autophagy of damaged mitochondria (mitophagy) represents a critical quality-control mechanism for maintaining cardiomyocytes homeostasis. Emerging evidence suggests exosomes modulate mitochondrial function in various injury models, including ischemic stroke [25] and traumatic brain injury [26]. Our work extends these findings by demonstrating that both EXO and EMPA-EXO potentiated mitophagy in H/R cardiomyocytes and I/R myocardium. Notably, we identify the mechanism wherein EXO/EMPA-EXO enhance PINK1/PARKIN-dependent mitophagy via ATAD3A upregulation. Our data reveal coordinated expression of ATAD3A and PINK1,

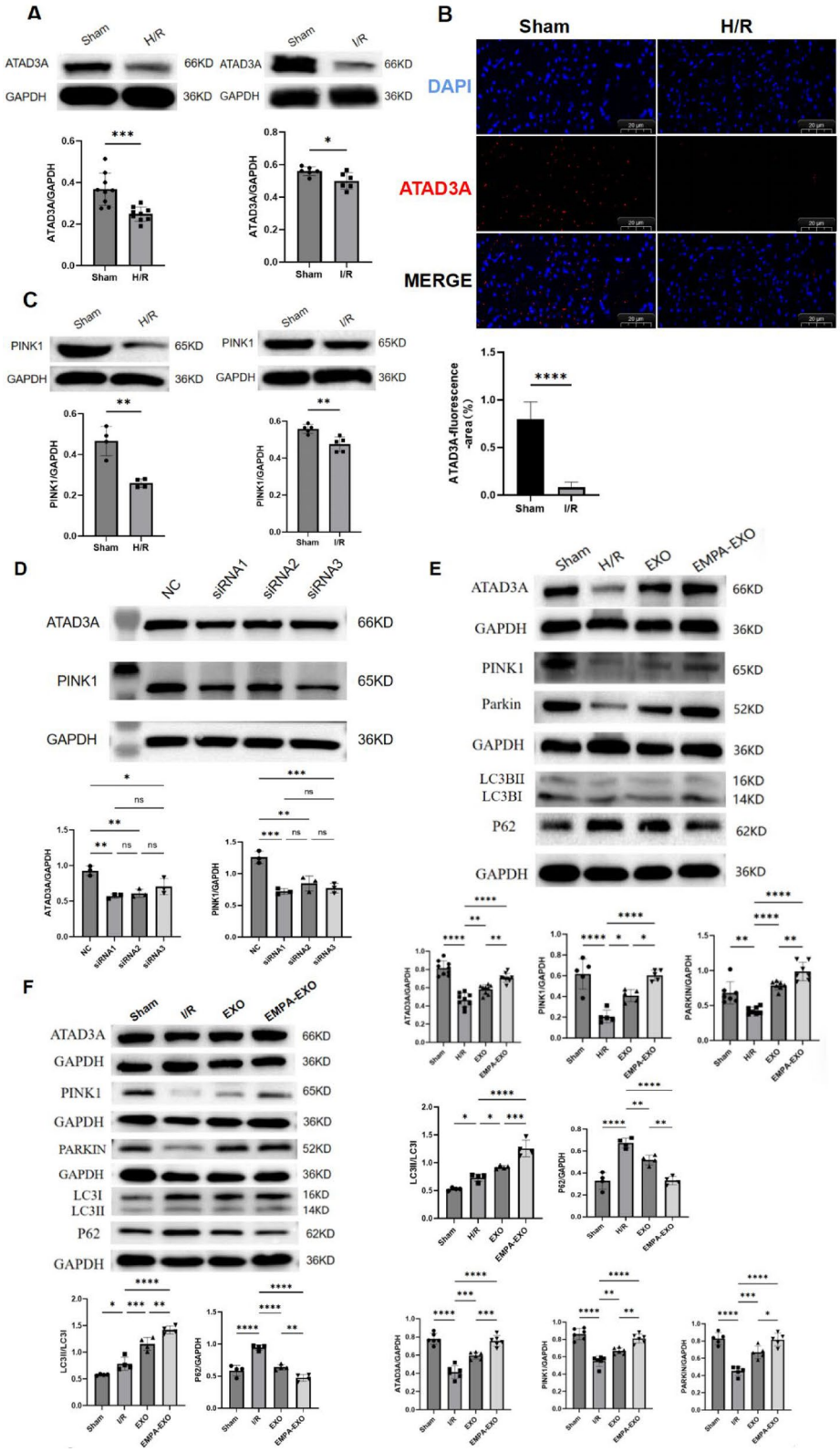

Fig. 5 EMPA-EXO Promoted Mitophagy in Ischemia-Reperfusion cardiomyocytes. **A**, **B** ATAD3A decreased in MIRI. **C** PINK1 decreased in MIRI. **D** PINK1 decreased along with the decline of ATAD3A in **cardiomyocytes. E** EMPA-EXO further promoted mitophagy in H/R NMCMs. **F**, **G** EMPA-EXO further promoted mitophagy in I/R mice myocardium. **H** TEM showed EMPA-EXO further promoted mitophagy I/R mice myocardium

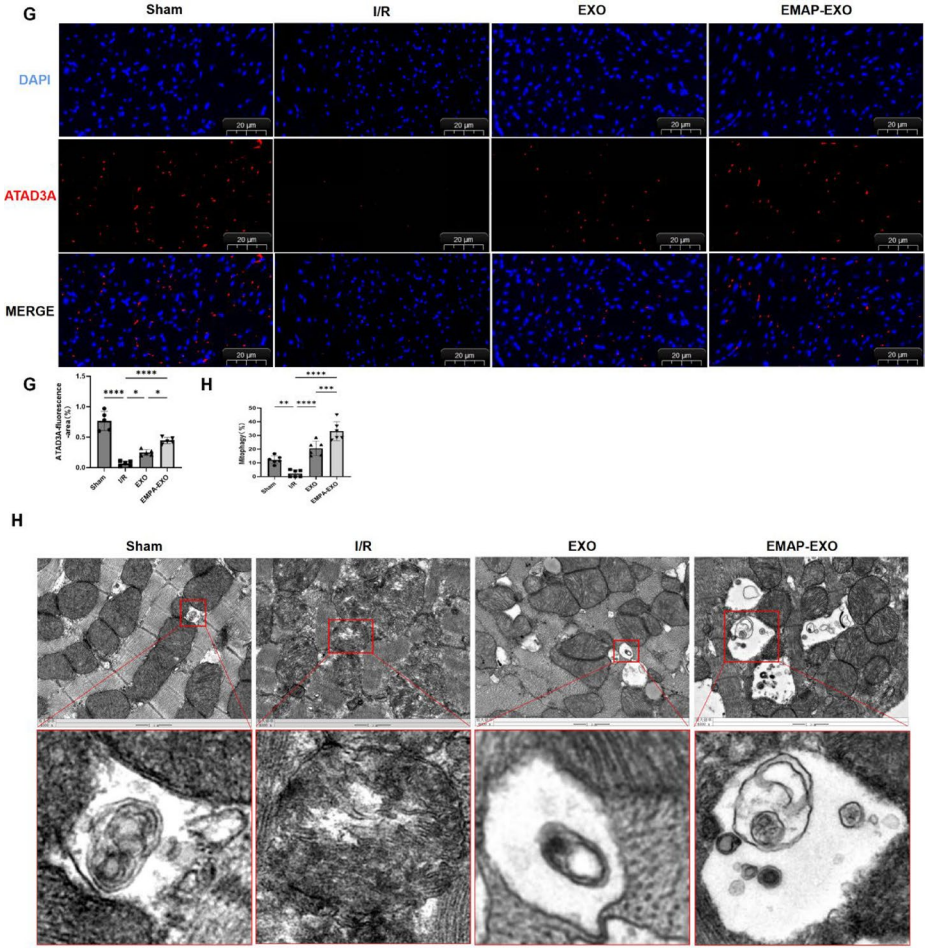

Fig. 5 (continued)

recapitulating the pattern observed in non-alcoholic fatty liver disease.

Exosomes have emerged as promising therapeutic agents for ICM due to their inherent biosafety, excellent biocompatibility, and low immunogenicity. However, clinical translation remains challenged by suboptimal production yields and variable therapeutic efficacy. Current optimization strategies include: biological preconditioning of MSCs with: Macrophage migration inhibitory factor (MIF) [27], and interferon-γ [28]. However, the application of exosome biological modification in clinical practice is rather limited. The method of treating MSCs with drugs is more direct and feasible in clinical practice. Tanshinone IIA could inhibit CCR2 activation, reduce monocyte infiltration and improve myocardial inflammation in I/R rats by up-regulating the content of UCMSCs-EXO miR-223-5p [8]. After Huang P et al. treated MSCs with atorvastatin, it was found that atorvastatin could significantly increase the content of lncRNA H19 in MSCS-EXO, and the therapeutic effect of promoting angiogenesis in rats with myocardial infarction and improving cardiomyocytes injury was more significant [9]. However, it is unknown whether the drug increases the production of exosomes. This study confirmed that empagliflozin could not only significantly enhance the efficacy of MSCs-EXO, but also significantly increased its yield.

Study limitations

The current research has some limitations. Firstly, The results of this experiment showed that EMPA-EXO significantly improved MIRI compared with EXO. However, due to experimental conditions issue, the specific components in EMPA-EXO and EXO were not further explored, which is the limitation of this experiment. Secondly, although we have demonstrated that EMPA can significantly increase the production of exosomes and have also examined the key factors involved in exosome generation, we have not further explored the underlying mechanism.

Conclusion

We found that EMPA could promote the production of EXO, and EMPA-EXO improved MIRI by enhancing PINK1/ Parkin-mediated mitophagy by increasing the expression of ATAD3A.

Supplementary Information

The online version contains supplementary material available at https://doi.org/10.1186/s13287-025-04715-6.

Supplementary Material 1.

Acknowledgments

Use of AI

The authors declare that they have not use AI-generated work in this manuscript.

Author contributions

Yuling Jing is responsible for designing experiments, doing experiments and writing article.; Ying Cai, Qiuting Li, Zaiyong Zheng, and Haiqiong Yang are responsible for doing experiments; Yang Yu is responsible for guiding the experiment and reviewing the article, and Chunxiang Zhang is responsible for designing experiments, guiding the experiment, and reviewing the article.

Funding

This work was supported by National Natural Science Foundation of China (Grant Nos. U23A20398;Grant Nos. 82030007), Noncommunicable Chronic Diseases-National Science and Technology Major Project(Grant Nos. 2024ZD0537707), Open Research Projects of the Ministry of Education Innovation Center for Basic Medical Research on Metabolic Cardiovascular Diseases (Grant Nos. xnykdxcxzx-2024-13).

Data availability

The data used and/or analyzed during the current study are available from the corresponding author on reasonable request.

Declarations

Ethics approval and consent to participate

All animal procedures conformed to Guide for Care and Use of Laboratory Animals published by US National Institute of Health (8th edition, 2011) and were approved by the Institutional Animal Care and Treatment Committee of Southwest Medical University, China.Consent for publication.Title of the approved project: Exosome in myocardial cell injury and ischemic heart disease. The ethical number is No. 2020255.

Competing interests

The authors declare no competing interests.

Author details

[1]Department of Cardiology, The Affiliated Hospital, Southwest Medical University, Luzhou 646000, Sichuan, China
[2]Key Laboratory of Medical Electrophysiology, Ministry of Education& Medical Electrophysiological Key Laboratory of Sichuan Province, Institute of Cardiovascular Research, Southwest Medical University, Luzhou 646000, Sichuan, China
[3]Basic Medicine Research Innovation Center for Cardiometabolic Diseases, Ministry of Education, Southwest Medical University, Luzhou 646000, Sichuan, China
[4]Nucleic Acid Medicine of Luzhou Key Laboratory, Southwest Medical University, Luzhou 646000, Sichuan, China

Received: 1 August 2025 / Accepted: 2 October 2025
Published online: 29 October 2025

References

1. Ferdinandy P, Andreadou I, Baxter GF, Bøtker HE, Davidson SM, Dobrev D, Gersh BJ, Heusch G, Lecour S, Ruiz-Meana M, Zuurbier CJ, Hausenloy DJ, Schulz R. Interaction of cardiovascular nonmodifiable risk Factors, comorbidities and comedications with Ischemia/Reperfusion injury and cardioprotection by Pharmacological treatments and ischemic conditioning. Pharmacol Rev. 2023;75(1):159–216.
2. Hade MD, Suire CN, Suo Z. Mesenchymal Stem Cell-Derived Exosomes: Applications in Regenerative Medicine. Cells. 2021;10(8):1959. https://doi.org/10.3390/cells10081959.
3. Fu X, Liu G, Halim A, Ju Y, Luo Q, Song AG. Mesenchymal stem cell migration and tissue repair. Cells. 2019;8(8):784. https://doi.org/10.3390/cells8080784.
4. Peng Y, Zhao JL, Peng ZY, Xu WF, Yu GL. Exosomal miR-25-3p from mesenchymal stem cells alleviates myocardial infarction by targeting pro-apoptotic proteins and EZH2. Cell Death Dis. 2020;11(5):317. https://doi.org/10.1038/s41419-020-2545-6. Erratum in: Cell Death Dis. 2020;11(9):791. doi: 10.1038/s41419-020-02996-8. Erratum in: Cell Death Dis. 2020;11(10):845. doi: 10.1038/s41419-020-03025-4.
5. Xiao C, Wang K, Xu Y, Hu H, Zhang N, Wang Y, Zhong Z, Zhao J, Li Q, Zhu D, Ke C, Zhong S, Wu X, Yu H, Zhu W, Chen J, Zhang J, Wang J, Hu X. Transplanted Mesenchymal Stem Cells Reduce Autophagic Flux in Infarcted Hearts via the Exosomal Transfer of miR-125b. Circ Res. 2018;123(5):564–578. https://doi.org/10.1161/CIRCRESAHA.118.312758.
6. Zhao J, Li X, Hu J, Chen F, Qiao S, Sun X, Gao L, Xie J, Xu B. Mesenchymal stromal cell-derived exosomes attenuate myocardial ischaemia-reperfusion injury through miR-182-regulated macrophage polarization. Cardiovasc Res. 2019;115(7):1205–16. https://doi.org/10.1093/cvr/cvz040.
7. Sun J, Shen H, Shao L, Teng X, Chen Y, Liu X, Yang Z, Shen Z. HIF-1α overexpression in mesenchymal stem cell-derived exosomes mediates cardioprotection in myocardial infarction by enhanced angiogenesis. Stem Cell Res Ther. 2020;11(1):373. https://doi.org/10.1186/s13287-020-01881-7.
8. Li S, Yang K, Cao W, Guo R, Liu Z, Zhang J, Fan A, Huang Y, Ma C, Li L, Fan G. Tanshinone IIA enhances the therapeutic efficacy of mesenchymal stem cells derived exosomes in myocardial ischemia/reperfusion injury via up-regulating miR-223-5p. J Control Release. 2023;358:13–26.
9. Huang P, Wang L, Li Q, Tian X, Xu J, Xu J, Xiong Y, Chen G, Qian H, Jin C, Yu Y, Cheng K, Qian L, Yang Y. Atorvastatin enhances the therapeutic efficacy of mesenchymal stem cells-derived exosomes in acute myocardial infarction via up-regulating long non-coding RNA H19. Cardiovasc Res. 2020;116(2):353–67. https://doi.org/10.1093/cvr/cvz139.
10. Anker SD, Butler J, Filippatos G, Ferreira JP, Bocchi E, Böhm M, Brunner-La Rocca HP, Choi DJ, Chopra V, Chuquiure-Valenzuela E, Giannetti N, Gomez-Mesa JE, Janssens S, Januzzi JL, Gonzalez-Juanatey JR, Merkely B, Nicholls SJ, Perrone SV, Piña IL, Ponikowski P, Senni M, Sim D, Spinar J, Squire I, Taddei S, Tsutsui H, Verma S, Vinereanu D, Zhang J, Carson P, Lam CSP, Marx N, Zeller C, Sattar N, Jamal W, Schnaidt S, Schnee JM, Brueckmann M, Pocock SJ, Zannad F, Packer M. EMPEROR-Preserved trial Investigators. Empagliflozin in heart failure with a preserved ejection fraction. N Engl J Med. 2021;385(16):1451–61. https://doi.org/10.1056/NEJMoa2107038.
11. Cai C, Guo Z, Chang X, Li Z, Wu F, He J, Cao T, Wang K, Shi N, Zhou H, Toan S, Muid D, Tan Y. Empagliflozin attenuates cardiac microvascular ischemia/reperfusion through activating the AMPKα1/ULK1/FUNDC1/mitophagy pathway. Redox Biol. 2022;52:102288. doi: 10.1016/j.redox.2022.102288. Epub 2022 Mar 18. Erratum in: Redox Biol. 2023;63:102738. https://doi.org/10.1016/j.redox.2023.102738.
12. Shimizu W, Kubota Y, Hoshika Y, Mozawa K, Tara S, Tokita Y, Yodogawa K, Iwasaki YK, Yamamoto T, Takano H, Tsukada Y, Asai K, Miyamoto M, Miyauchi Y, Kodani E, Ishikawa M, Maruyama M, Ogano M, Tanabe J. EMBODY trial investigators. Effects of empagliflozin versus placebo on cardiac sympathetic activity in acute myocardial infarction patients with type 2 diabetes mellitus: the EMBODY trial. Cardiovasc Diabetol. 2020;19(1):148. https://doi.org/10.1186/s12933-020-01127-z.
13. Yang CC, Chen YL, Sung PH, Chiang JY, Chen CH, Li YC, Yip HK. Repeated administration of adipose-derived mesenchymal stem cells added on beneficial effects of empagliflozin on protecting renal function in diabetic kidney disease rat. Biomed J. 2024;47(2):100613. https://doi.org/10.1016/j.bj.2023.100613.
14. Chi B, Zou A, Mao L, Cai D, Xiao T, Wang Y, Wang Q, Ji Y, Sun L. Empagliflozin-Pretreated mesenchymal stem Cell-Derived small extracellular vesicles attenuated heart injury. Oxid Med Cell Longev. 2023;2023:7747727. https://doi.org/10.1155/2023/7747727.

15. Xie XQ, Yang Y, Wang Q, Liu HF, Fang XY, Li CL, Jiang YZ, Wang S, Zhao HY, Miao JY, Ding SS, Liu XD, Yao XH, Yang WT, Jiang J, Shao ZM, Jin G, Bian XW. Targeting ATAD3A-PINK1-mitophagy axis overcomes chemoimmunotherapy resistance by redirecting PD-L1 to mitochondria. Cell Res. 2023;33(3):215–28. https://doi.org/10.1038/s41422-022-00766-z.
16. Li X, Guan L, Liu Z, Du Z, Yuan Q, Zhou F, Yang X, Lv M, Lv L. Ubiquitination of ATAD3A by TRIM25 exacerbates cerebral ischemia-reperfusion injury via regulating PINK1/Parkin signaling pathway-mediated mitophagy. Free Radic Biol Med. 2024;224:757–69.
17. Wu H, Wang T, Liu Y, Li X, Xu S, Wu C, Zou H, Cao M, Jin G, Lang J, Wang B, Liu B, Luo X, Xu C. Mitophagy promotes Sorafenib resistance through hypoxia-inducible ATAD3A dependent axis. J Exp Clin Cancer Res. 2020;39(1):274. https://doi.org/10.1186/s13046-020-01768-8.
18. Chen L, Li Y, Sottas C, et al. Loss of mitochondrial ATPase ATAD3A contributes to nonalcoholic fatty liver disease through accumulation of lipids and damaged mitochondria [J]. J Biol Chem. 2022;298(6):102008. https://doi.org/10.1016/j.jbc.2022.102008.
19. Yu Y, Yang H, Li Q, Ding N, Gao J, Qiao G, Feng J, Zhang X, Wu J, Yu Y, Zhou X, Wang X, Zhang C. Stress-enhanced cardiac LncRNA morrbid protects hearts from acute myocardial infarction. JCI Insight. 2023;8(16):e165568. https://doi.org/10.1172/jci.insight.165568.
20. Sun XH, Wang X, Zhang Y, et al. Exosomes of bone-marrow stromal cells inhibit cardiomyocyte apoptosis under ischemic and hypoxic conditions via miR-486-5p targeting the PTEN/PI3K/AKT signaling pathway [J]. Thromb Res. 2019;177:23–32.
21. Li T, Gu J, Yang O, Wang J, Wang Y, Kong J. Bone marrow mesenchymal stem Cell-Derived Exosomal miRNA-29c decreases cardiac Ischemia/Reperfusion injury through Inhibition of excessive autophagy via the PTEN/Akt/mTOR signaling pathway. Circ J. 2020;84(8):1304–11. https://doi.org/10.1253/circj.CJ-19-1060.
22. Yue R, Lu S, Luo Y, Zeng J, Liang H, Qin D, Wang X, Wang T, Pu J, Hu H. Mesenchymal stem cell-derived Exosomal microRNA-182-5p alleviates myocardial ischemia/reperfusion injury by targeting GSDMD in mice. Cell Death Discov. 2022;8(1):202. https://doi.org/10.1038/s41420-022-00909-6.
23. Song Y, Wang B, Zhu X, Hu J, Sun J, Xuan J, Ge Z. Human umbilical cord blood-derived MSCs exosome attenuate myocardial injury by inhibiting ferroptosis in acute myocardial infarction mice. Cell Biol Toxicol. 2021;37(1):51–64. https://doi.org/10.1007/s10565-020-09530-8.
24. Paradies G, Paradies V, Ruggiero FM, Petrosillo G. Mitochondrial bioenergetics and Cardiolipin alterations in myocardial ischemia-reperfusion injury: implications for Pharmacological cardioprotection. Am J Physiol Heart Circ Physiol. 2018;315(5):H1341–52. https://doi.org/10.1152/ajpheart.00028.2018.
25. Zhu X, Liu Q, Zhu F, Jiang R, Lu Z, Wang C, Gong P, Yao Q, Xia T, Sun J, Ju F, Wang D, Sun R, Zhou Y, You B, Shi W. An engineered cellular carrier delivers miR-138-5p to enhance mitophagy and protect hypoxic-injured neurons via the DNMT3A/Rhebl1 axis. Acta Biomater. 2024;186:424–38.
26. Zhang L, Lin Y, Bai W, Sun L, Tian M. Human umbilical cord mesenchymal stem cell-derived exosome suppresses programmed cell death in traumatic brain injury via PINK1/Parkin-mediated mitophagy. CNS Neurosci Ther. 2023;29(8):2236–58. https://doi.org/10.1111/cns.14159.
27. Zhu W, Sun L, Zhao P, Liu Y, Zhang J, Zhang Y, Hong Y, Zhu Y, Lu Y, Zhao W, Chen X, Zhang F. Macrophage migration inhibitory factor facilitates the therapeutic efficacy of mesenchymal stem cells derived exosomes in acute myocardial infarction through upregulating miR-133a-3p. J Nanobiotechnol. 2021;19(1):61. https://doi.org/10.1186/s12951-021-00808-5.
28. Zhang J, Lu Y, Mao Y, Yu Y, Wu T, Zhao W, Zhu Y, Zhao P, Zhang F. IFN-γ enhances the efficacy of mesenchymal stromal cell-derived exosomes via miR-21 in myocardial infarction rats. Stem Cell Res Ther. 2022;13(1):333. https://doi.org/10.1186/s13287-022-02984-z.

Publisher's Note